

# A study of reaction-diffusion problems for domains bounded by periodic source/sink distributions on planar surfaces: an application to microelectrode processes

S.K. Lucas & H.A. Stone

*Division of Applied Sciences, Harvard University, Cambridge, MA 02138 U.S.A.*

## Abstract

Reaction-diffusion problems that are characterized by the presence of isolated sources along bounding surfaces of a liquid-filled container arise in typical electrochemical applications utilizing arrays of microelectrodes, in modelling corrosion of surfaces, and in models of catalysis. The mathematical treatment of the associated mass transport problem is difficult due to the character of the resulting mixed boundary value problem, whereby reaction occurs at isolated sites on boundaries with the remainder of the surface treated as insulating. Here we examine the case of steady-state transport to periodic arrays of circular disc-shaped microelectrodes mounted flush in an infinite, insulating planar boundary. Numerical procedures based upon integral equation methods are developed with an appropriate periodic Green's function, whose slow convergence rate is improved by the method of Ewald. Results are presented for surface flux as a function of bulk and surface reaction rates and surface coverage.

## 1 Introduction

Mass transport coupling diffusion, surface and/or bulk chemical reactions, and species migration in external fields occurs in a wide variety of physical situations, including electrochemistry, catalysis, corrosion, colloidal suspensions, protein binding, etc. The transport process is frequently controlled by surface chemical reactions or by charge distributed along the bounding surfaces. In general, such bounding surfaces are heterogeneous and so surface properties (e.g. reactivity) vary spatially. For example, electrochemical devices consisting of arrays of microelectrodes (Wightman & Wipf [8]) have

the geometric feature that surface chemical reactions occur on many distributed regions, or patches, on an otherwise unreactive substrate. Due to the small size of the microelectrodes, steady state conditions are generally reached quickly. Although mass transfer to an isolated surface patch has been studied for a variety of surface geometries (e.g. strips, hemispheres, discs, and rings) (Brett & Brett [4]), a surface with a periodic array of active sites has received much less attention. Here, we study the steady state reaction-diffusion problem for a stagnant fluid bounded by a plane which is covered by a periodic array of circular reactive sites.

## 2 Formulation

Consider a periodic array of circular microelectrodes denoted  $S_E$  distributed over an otherwise insulating boundary  $S_P$  at  $z = 0$  as illustrated in Figure 1(a). An electrolytic solution fills the entire volume  $z > 0$  above the plane, and we are interested in calculating the steady state current to the surface due to oxidation-reduction processes that occur on the surface of the electrodes while allowing for chemical regeneration in the bulk. The flux of a given oxidized (or reduced) chemical species to the electrode is proportional to the measured electrode current, and so we seek a solution for the concentration flux of the chemical species. We assume that there is no fluid motion, and so following Phillips [6,7] and Bender & Stone [2], the steady state reaction-diffusion equation for the problem can be written in dimensionless form as

$$\nabla^2 \phi = \alpha^2 \phi \quad \text{with} \quad \begin{cases} \phi = 1 + \frac{1}{K} \frac{\partial \phi}{\partial z} & \text{on } z = 0, \mathbf{x} \in S_E, \\ \frac{\partial \phi}{\partial z} = 0 & \text{on } z = 0, \mathbf{x} \in S_P, \\ \phi \rightarrow 0 & \text{as } z \rightarrow \infty, \end{cases} \quad (1)$$

where  $\phi(\mathbf{x})$  is the dimensionless concentration in the fluid,  $\alpha^2$  is a constant representing the ratio of bulk species regeneration relative to diffusion,  $K$  is a constant representing the ratio of surface reaction rate at the electrode surface relative to diffusion in the bulk, and  $\mathbf{x}$  denotes the position vector. In this study we will assume  $K = \infty$ , the limit at which surface reaction is instantaneous. We shall assume the periodic cell on the surface is rectangular of size  $(2l_1 \times 2l_2)$ , with circular microelectrodes of radius one centered within the periodic cells. Because of the periodicity, we only need to determine the solution within a single cell. Rather than calculate the concentration  $\phi$  directly, we are more interested in the flux  $\partial\phi/\partial z$  at  $z = 0$ . Once the flux distribution has been calculated, the total dimensionless flux to a single electrode is determined by integrating  $\partial\phi/\partial z$  over the surface  $S_E$ , which is proportional to the measured current through the electrode. Since we are only interested in finding the flux distribution over the electrode,

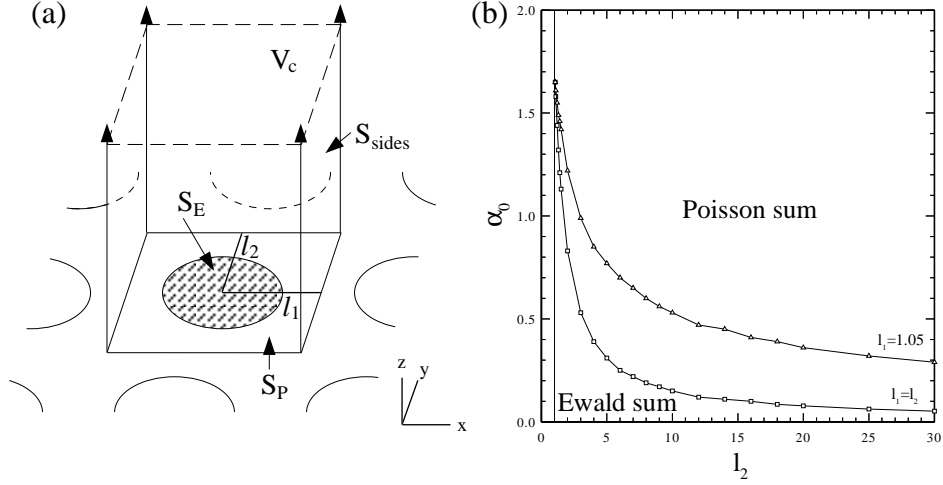


Figure 1: (a) Geometry of the volume above a periodic cell on a surface periodically covered with discs. (b) Value of  $\alpha$  at which the Poisson and Ewald summations take the same amount of CPU time versus  $l_2$  for the two cases  $l_1 = l_2$  and  $l_1 = 1.05$ .

the volume of application of (1) is the infinite half-space, and (1) is linear, an integral equation approach is ideal, as opposed to finite element or finite difference techniques. The solution approach is standard, although some of the details necessary to treat the periodic surface condition and numerically calculate the flux accurately require some care.

## 2.1 Integral Equation Derivation

Due to the periodic nature of the problem, we have that  $\phi(\mathbf{x}) = \phi(\mathbf{x} + \mathbf{x}_p)$ , where  $\mathbf{x}_p = (2l_1m_1, 2l_2m_2, 0)$  with  $m_1, m_2 = 0, \pm 1, \pm 2, \dots$  is the periodic vector. Rather than solving for  $\phi$  throughout the entire volume, we may treat instead the volume above a single periodic cell (see Figure 1(a)), with volume  $V_c$  and boundary  $S_c = S_E \cup S_P \cup S_\infty \cup S_{sides}$ . The surface  $S_\infty$  is the ‘cap’ of the volume at  $z = \infty$ . A boundary integral formulation of (1) with the given boundary and periodicity conditions gives us that the flux satisfies the integral equation of the first kind

$$1 = \int_{S_E} 2G(\mathbf{x} - \mathbf{y})\phi'(\mathbf{x}) dS(\mathbf{x}), \quad \mathbf{y} \in S_E, \quad (2)$$

where we have written  $\phi'$  for  $\partial\phi/\partial z$ . The Green’s function  $G$  is the solution of

$$\nabla_{\mathbf{x}}^2 G(\mathbf{x} - \mathbf{y}) = \alpha^2 G(\mathbf{x} - \mathbf{y}) + \sum_{m_1=-\infty}^{\infty} \sum_{m_2=-\infty}^{\infty} \delta(\mathbf{x} - \mathbf{y} - \mathbf{x}_p) \quad (3)$$

$$\text{with } G \rightarrow 0 \text{ as } |x_3 - y_3| \rightarrow \infty,$$

where the Laplacian operator is with respect to the variable  $\mathbf{x}$ , and  $x_3 - y_3$  is the  $z$ -component of  $\mathbf{x} - \mathbf{y}$ . The Green's function can be found by solving (3) using 2D Fourier transforms. Since from (2) both  $\mathbf{x}$  and  $\mathbf{y} \in S_E$ ,  $x_3 - y_3 = 0$  here, and so

$$G(\mathbf{x} - \mathbf{y}) = - \sum_m \frac{\exp\{-2\pi i \mathbf{h}_m \cdot \mathbf{R}\}}{8l_1 l_2 \sqrt{4\pi^2 \mathbf{h}_m^2 + \alpha^2}}, \text{ with } \begin{cases} \mathbf{R} = \mathbf{x} - \mathbf{y}, \\ \mathbf{h}_m = (m_1/2l_1, m_2/2l_2), \end{cases} \quad (4)$$

and  $\sum_m$  denotes the doubly infinite summation over  $m_1$  and  $m_2$ .

## 2.2 Accelerating Convergence of the Green's Function

The form of the Green's function given in (4) converges very slowly. Convergence may be accelerated by applying Poisson's summation formula (Barton [1]), which gives

$$G(\mathbf{R}) = - \sum_m \frac{e^{-\alpha k}}{4\pi k}, \quad k = \sqrt{(R_1 - 2m_1 l_1)^2 + (R_2 - 2m_2 l_2)^2}. \quad (5)$$

This can be recognized as a distribution of the free space Green's function used in Bender & Stone [2]. Unfortunately, for small  $\alpha$ , (5) also converges slowly. Another option is to utilize the method of Ewald (Nijboer & De Wette [5]), which converts (4) to

$$\begin{aligned} G(\mathbf{R}) = & -\frac{1}{4l_1 l_2} \sum_m e^{\pi i \left(\frac{m_1 R_1}{l_1} + \frac{m_2 R_2}{l_2}\right)} \frac{\text{erfc}(c\sqrt{A})}{\sqrt{A}} \\ & - \frac{1}{4\pi} \sum_m \frac{1}{k} \left[ e^{k\alpha} \text{erfc}\left(\frac{k}{2c} + \alpha c\right) + e^{-k\alpha} \text{erfc}\left(\frac{k}{2c} - \alpha c\right) \right], \end{aligned} \quad (6)$$

where

$$k = \sqrt{(R_1 - 2l_1 m_1)^2 + (R_2 - 2l_2 m_2)^2}, \quad A = \pi^2 \left\{ \left(\frac{m_1}{l_1}\right)^2 + \left(\frac{m_2}{l_2}\right)^2 \right\} + \alpha^2. \quad (7)$$

The arbitrary parameter  $c$  is chosen to obtain the best convergence for  $G(\mathbf{R})$ . Since  $\text{erfc}(x) = O(e^{-x^2})$  for  $x \gg 1$ , we can balance the convergence rates of the complimentary error function terms in (6) to arrive at the estimate

$$c = \sqrt{\frac{l_1 l_2}{\pi}}. \quad (8)$$

While additional terms of the Ewald sum in (6) are  $O(e^{-m^2})$ , which converge faster than the additional terms of the exponentials in (5),  $O(e^{-m})$ , the Ewald sum involves two complimentary error functions, which take much longer to numerically evaluate than an exponential. To decide which of (5) or (6) to use, we calculate the Green's function for a specified  $\alpha$ ,  $l_1$ , and  $l_2$

to eight digit accuracy at  $10^5$  representative points, and choose the fastest of the two methods. Figure 1(b) shows curves of the critical value of  $\alpha$  for specific  $l_1, l_2$  at which the two sums are identical, and so indicates which summation should be used for other  $\alpha$  values. Above the curves, the exponential sum (5) is best; below, the Ewald sum (6) is superior. The trigonometric form (4) is never used.

### 3 Solution Method

Due to the circular geometry of  $S_E$ , we express the unknown  $\partial\phi/\partial z = \phi'$  in polar coordinates. Symmetry implies we only need to determine  $\phi'$  in the first quadrant. We divide the rectangle  $[0, 1] \times [0, \pi/2]$  in polar coordinates into  $M \times N$  elements and assume  $\phi'$  varies quadratically over each element in  $r$  and  $\theta$ . Collocation points are placed at node points of the quadratic elements, which leads to a linear system of equations that is solved for  $\phi'$  as in standard boundary element techniques (Brebbia *et al.* [3]). Several sophisticated numerical techniques are used to calculate accurately and efficiently the required 2D integrals.

For  $K = \infty$ , it can be shown by an asymptotic analysis of (1) that  $\phi'$  has an inverse square root singularity near  $r = 1$ , the outer edge of the disc. This significantly degrades performance of numerical techniques to find  $\phi'$ , and so we replace  $\phi'$  in (4) by  $\hat{\phi}'/\sqrt{1-r}$ , and solve for  $\hat{\phi}'$ , which is a smooth function. The assumption of an inverse square root singularity in the flux at the edge of the disc accelerates convergence of the numerical solution significantly, and it was found that  $5 \times 5$  quadratic elements are sufficient to capture the variations of  $\hat{\phi}'$  in both the  $r$  and  $\theta$  directions such that the total flux over the disc is accurate to at least three significant digits. The system of equations to be solved has 96 unknowns, and takes at least 10 minutes on a Sun Sparc 10 workstation for cases with  $l_1 = l_2$ . This performance indicates the relatively high cost of calculating the periodic Green's function.

### 4 Results

Figure 2(a) shows total flux per disc  $\int_{S_E} \phi' dS$  versus  $l_1$  with  $l_1 = l_2$  for various values of  $\alpha$ . The horizontal dashed lines represent the flux for a single disc on the insulating surface. We see that as  $l_1(=l_2)$  increases, the flux per disc approaches that for a single disc. As  $\alpha$  increases, the approach to the single disc result is more rapid, since for large  $\alpha$ , bulk regeneration of reactants within the fluids is large with respect to diffusion, and so most reaction occurs close to the electrode, and in fact occurs within a boundary layer  $O(\alpha^{-1})$  above the disc. Furthermore, as  $\alpha$  increases, the size of the periodic cell such that individual electrodes have no effect on each other decreases. For small  $\alpha$ , diffusion dominates, and the restriction of each electrode only having access to the reactants above its own periodic cell

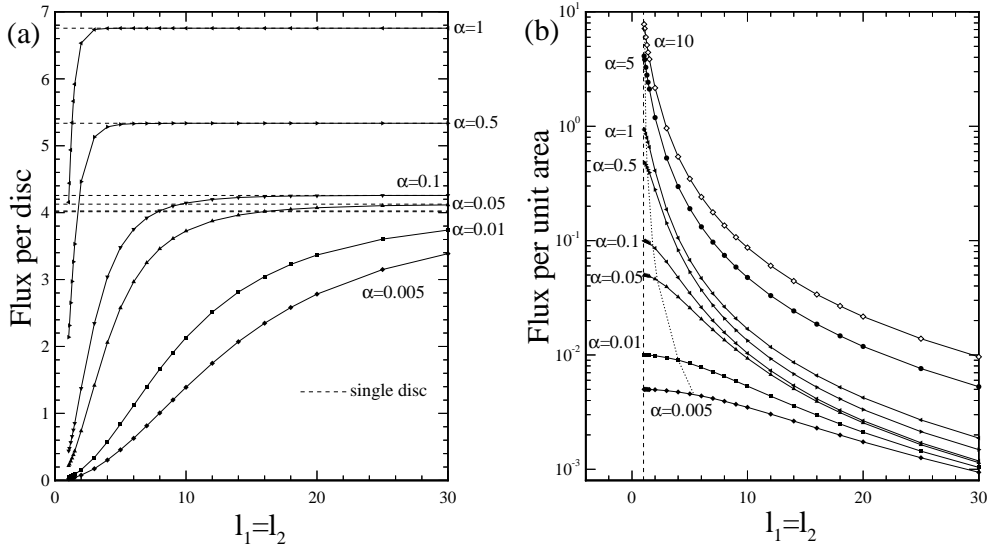


Figure 2: (a) Flux per disc, and (b) Flux per unit area, versus  $l_1 = l_2$  for various values of  $\alpha$  and  $K = \infty$ . The dotted line in (b) represents the value of  $l_1 = l_2$  at which the flux per unit area is 90% of its value at  $l_1 = l_2 = 1.05$ .

becomes more important. We can observe that for low  $\alpha$ , even for large values of  $l_1 (= l_2)$ , the flux per disc is significantly below the single disc result, showing the large influence of electrodes on their neighbours when diffusion dominates.

Figure 2(b) shows the flux per unit area versus  $l_1 (= l_2)$ , where the flux per unit area is defined as the flux for individual discs divided by the area of the periodic cell. This measure provides a better idea of the overall performance of the periodic array. For large  $l_1 = l_2$ , the slopes of the curves are  $-2$ . Since for large  $l_1 = l_2$  the flux per disc approaches a constant (the single disc result), and as the area of the periodic cell increases as the square of the cell lengths  $l_1 = l_2$ , the factor of  $-2$  is as expected. We have also included in Figure 2(b) a dotted line across the various  $\alpha$  curves. The dotted line is the value of  $l_1 = l_2$  at which the flux per unit area is 90% of its value at  $l_1 = l_2 = 1.05$ , and we can see that as  $\alpha$  decreases, this value increases. Curves such as this show how additional effort (placing electrodes closer together) gives a much smaller additional return in flux for small  $\alpha$ .

Figure 3(a) shows the variation of the local flux distribution  $\phi'$  at  $r = 0.9$  as a function of the angle  $\theta$  for several periodic cell sizes,  $\alpha = 0.01$ . Curves have been scaled by the minimum flux on the curve, at  $\theta = 0$ , so comparisons of variation can be made. We see that the variation in  $\phi'$  drops dramatically as  $l_1 = l_2$  increases, and is virtually zero for  $l_1 = l_2 \geq 5$ . Since the flux per disc is still well below the single disc result, we conclude that variation

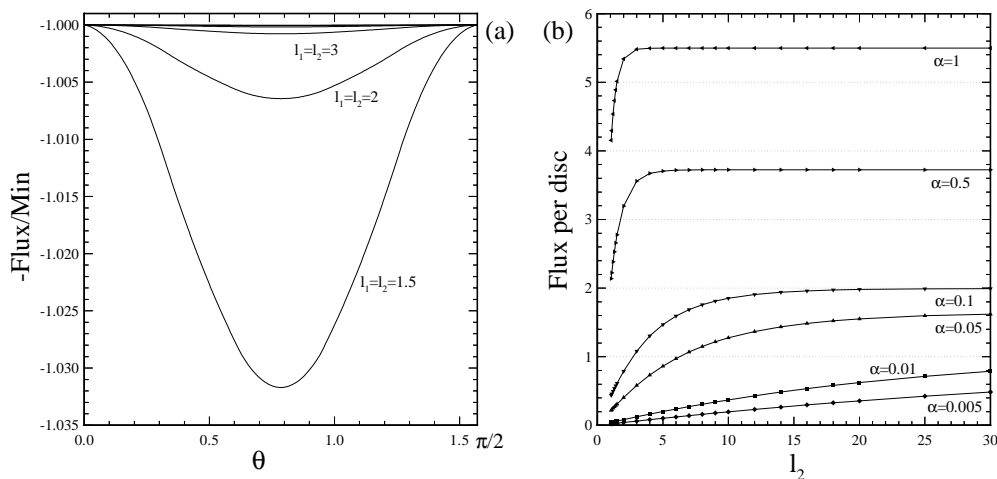


Figure 3: (a)  $\phi'$  versus  $\theta$  along  $r = 0.9$  for  $\alpha = 0.01$ ,  $K = \infty$ , and  $l_1 = l_2 = 1.05, 2, 3, 4, 5, 6$ . The curves are scaled with respect to  $\phi'$  at  $\theta = 0$ . (b) Flux per disc versus  $l_2$  for  $l_1 = 1.05$ , various  $\alpha$ .

of  $\phi'$  in the  $\theta$  direction is primarily due to interaction with the closest electrodes. When the periodic cell size increases, the lowered flux is due to reactants only being available from the volume above each periodic cell. This observation explains the observable point of inflexion in the flux curves of Figure 2(a) for small  $\alpha$ , where the additional interaction of electrodes becomes important for  $l_1 = l_2 < 5$ .

Figure 3(b) shows the flux per disc results rectangular periodic cells, where now  $l_1$  has been fixed and  $l_2$  varies. The final flux values for large  $l_2$  are smaller than for  $l_1 = l_2$  since there is more interaction between electrodes, and we also observe that the inflexions in the curves of Figure 2(a) are no longer apparent; since  $l_1 = 1.05$  in Figure 3(b), discs always respond close together, and angular variations in the flux will not be lost.

## 5 Conclusion

Bender & Stone [2] developed an integral equation solution for the single disc steady state microelectrode problem, and produced accurate numerical results. Here, we have extended that study to the problem of a periodic array of microelectrodes, and investigated the effects of varying the periodic cell sizes. Once the inverse square root singularity in the solution was identified, quadratic boundary elements gave us very accurate numerical results. However, a significant amount of analysis was required to form a Green's function that could be calculated efficiently.

A more comprehensive version of this paper is available from the authors

which gives more detail on the formulation of the problem, development of Green's functions, and other implementation details including the use of sophisticated integration routines. This paper also addresses the case of finite  $K$ , where the reaction rate on the surface of the microelectrodes is not instantaneous. Several other extensions to this problem are possible, including investigation of other microelectrode shapes which may give higher flux results for the same electrode to surface ratio, or random arrays of microelectrodes, which more realistically model this problem's catalytic analog.

### Acknowledgements

We gratefully acknowledge NSF-PYI Award CT5-8957043 (to HAS) and the MERCK Foundation for funding this study. We thank Ms. Radica Sipic for her input in the formulation of this problem, and Professors Ali Nadim and Ashok Sangani for helpful conversations and discussion on Ewald sums.

### References

1. Barton, G. *Elements of Green's functions and propagation*, Oxford University Press, Oxford, 1989.
2. Bender, M.A. & Stone, H.A. An integral equation approach to the study of the steady state current at surface microelectrodes, *J. Electroanal. Chem.*, 1993, **351**, 29-55.
3. Brebbia, C.A., Telles, J.C.F. & Wrobel, L.C. *Boundary element techniques: theory and applications in engineering*, Springer-Verlag, Berlin, 1984.
4. Brett, C.M.A. & Brett, A.M.O. *Electrochemistry principles, methods, and applications*, Oxford University Press, Oxford, 1993.
5. Nijboer, B.R.A. & De Wette, F.W. On the calculation of lattice sums, *Physica*, 1957, **23**, 309-321.
6. Phillips, C.G. The steady-state current for a microelectrode near diffusion-limited conditions, *J. Electroanal. Chem.*, 1990, **291**, 251-256.
7. Phillips, C.G. The steady, diffusion-limited current at a disk microelectrode with a first order EC' reaction, *J. Electroanal. Chem.*, 1990, **296**, 255-258.
8. Wightman, R.M. & Wipf, D.O. Voltammetry at ultramicroelectrodes, *Electroanal. Chem.*, 1989, **15**, 267-353.